Journal of Advanced Research 24 (2020) 167–173

Contents lists available at ScienceDirect

Journal of Advanced Research

journal homepage: www.elsevier.com/locate/jare

The similarities and differences of different plane solitons controlled by (3 + 1) – Dimensional coupled variable coefficient system

Xiaoyan Liu [a], Qin Zhou [b], Anjan Biswas [c,d,e,f], Abdullah Kamis Alzahrani [d], Wenjun Liu [a,*]

[a] State Key Laboratory of Information Photonics and Optical Communications, and School of Science, Beijing University of Posts and Telecommunications, P.O. Box 122, Beijing 100876, China
[b] School of Electronics and Information Engineering, Wuhan Donghu University, Wuhan 430212, China
[c] Department of Physics, Chemistry and Mathematics, Alabama A|&M University, Normal, AL 35762-7500, USA
[d] Department of Mathematics, King Abdulaziz University, Jeddah 21589, Saudi Arabia
[e] Department of Applied Mathematics, National Research Nuclear University, Kashirskoe Shosse, Moscow 115409, Russian Federation
[f] Department of Mathematics and Statistics, Tshwane University of Technology, Pretoria 0008, South Africa

GRAPHICAL ABSTRACT

Periodic parabolic solitons with different energies have been presented. The purpose of changing the period and span of the parabolic solitons has been achieved by adjusting the corresponding parameters.

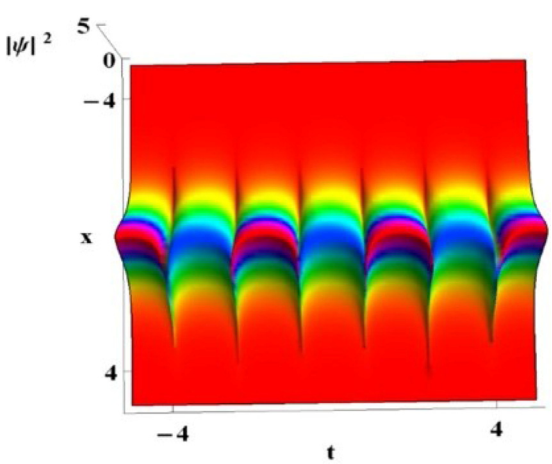

ARTICLE INFO

Article history:
Received 19 February 2020
Revised 3 April 2020
Accepted 3 April 2020
Available online 13 April 2020

ABSTRACT

In this paper, a system with controllable parameters for describing the evolution of polarization modes in nonlinear fibers is studied. Using the Horita's method, the coupled nonlinear Schrödinger equations are transformed into the bilinear equations, and the one- and two- bright soliton solutions of system (3) are obtained. Then, the influencing factors on velocity and intensity in the process of soliton transmission are analyzed. The fusion, splitting and deformation of the solitons caused by their interactions are discussed.

Peer review under responsibility of Cairo University.
* Corresponding author.
E-mail addresses: qinzhou@whu.edu.cn (Q. Zhou), jungliu@bupt.edu.cn (W. Liu).

https://doi.org/10.1016/j.jare.2020.04.003
2090-1232/

Finally, a method for adjusting the inconsistencies of sine-wave soliton transmission is given. The conclusions of this paper may be helpful for the related research of wavelength division multiplexing systems.

Keywords:
Soliton transmission
Horita's method
Soliton solutions
Coupled nonlinear Schrödinger equations

Introduction

In fiber optics, some studies have been conducted on the traditional optical pulse transmission model [1–10]. With the further study of fiber optics, scientists have extended the study of the traditional optical pulse transmission model nonlinear Schrödinger equation (NLSE) in optical fiber to multi-dimensional NLSE, coupled NLSE (CNLSE) in birefringent fiber, N-coupled NLSE in wavelength division multiplexing system and variable coefficient NLSE in non-uniform fiber [11–17]. As one of the basic theoretical models for describing nonlinear phenomena, the CNLSEs are widely used in such fields as biophysics, condensed matter physics and nonlinear optics [18–21]. The classic CNLSE is:

$$\begin{aligned} &iq_{1t} + c_1 q_{1xx} + \omega\left(|q_1|^2 + \alpha_1 |q_2|^2\right) q_1 = 0, \\ &iq_{2t} + c_2 q_{2xx} + \omega\left(\alpha_2 |q_1|^2 + |q_2|^2\right) q_2 = 0. \end{aligned} \tag{1}$$

where q_1 and q_2 represent slowly varying amplitudes of two fiber modes, they are complex functions with respect to scale distance x and time t [22–25]. The System (1) includes both self-phase modulation and cross-phase modulation, α_1 and α_2 are cross-phase modulation coefficients, c_1 and c_2 are the dispersion coefficients of the two wave packets, respectively. For System (1), its exact solutions and soliton transmission characteristics have been studied. By introducing Hirota's method, the bright soliton and dark soliton solutions of System (1) have been obtained under the conditions of $c_1 = c_2 = 1$ and $\alpha_1 = \alpha_2 = 1$ [26]. The periodic solutions of the systems extended to the N-components have been expressed, and the inelastic interactions caused by intensity redistribution and separation distance have been analyzed [27].

The soliton solution of the high-dimensional CNLEs are more complicated in structure, so that they can produce more abundant new physical phenomena. Therefore, the (1 + 1)-dimensional CNLSEs have been extended to the (2 + 1)-dimensional CNLSEs [28].

$$\begin{aligned} &i\psi_t + \gamma(\psi_{xx} + \psi_{yy}) + \sigma\left(|\psi|^2 + |\phi|^2\right)\psi &= 0, \\ &i\phi_t + \gamma(\phi_{xx} + \phi_{yy}) + \sigma\left(|\psi|^2 + |\phi|^2\right)\phi &= 0. \end{aligned} \tag{2}$$

System (2) controls the existence and stability of the space vector solitons, and the solutions of System (2) are derived under the condition of $\gamma = \sigma = 1$ parameters, and the elastic and inelastic interactions between two parallel bright solitons have been analyzed [28]. In reference [29], N-components (2 + 1)-dimensional CNLSEs have been discussed, which describe the evolution of polarization modes in nonlinear fibers. However, in the process of practical application, some special phenomena such as local defects and damages cannot be explained by constant coefficient system model in optical fiber, which always have an important impact on the optical soliton transmissions and dynamic behavior [30]. Therefore, the variable coefficient CNLSEs have much practical significance and research value. When γ and σ develop into $\gamma(t)$ and $\sigma(t)$ respectively, the bright and dark analytic soliton solutions of the changed System (2) and their related properties have been reported [30,31].

Further, the higher the dimension of the nonlinear equation, the more accurately the equation can describe the actual physical phenomenon, so that the CNLSE is extended from (2 + 1) dimension to (3 + 1) dimension [32]. Not only that, finding the exact solutions of the variable coefficient CNLES, especially the soliton solutions, has always been a topic of great interest to mathematicians and physicists. Consider the above factors, we will focus on the following (3 + 1)-dimensional variable coefficient system model [32–35],

$$\begin{aligned} &i\psi_t + \beta(t)\left[\psi_{xx} + \psi_{yy} + \psi_{zz}\right] + \delta(t)\left(|\psi|^2 + |\phi|^2\right)\psi = 0, \\ &i\phi_t + \gamma(t)\left[\phi_{xx} + \phi_{yy} + \phi_{zz}\right] + \omega(t)\left(|\psi|^2 + |\phi|^2\right)\phi = 0, \end{aligned} \tag{3}$$

where $\beta(t), \delta(t), \gamma(t)$ and $\omega(t)$ are all perturbed real functions. When they are all constants, the bright soliton solutions of the constant coefficient $(3+1)$-dimensional CNLSE has been solved in Ref. [33]. Subsequently, the dark soliton solutions have been derived under the constraints of $\delta(t) = \omega(t) = -\beta(t) = -\lambda$ and $\gamma(t) = \beta(t) = \lambda$ in Ref. [34]. The variable-coefficient dark solitons of the system (3) with the constraints $\beta(t) = \gamma(t)$and$\delta(t) = \omega(t)$, and their different transmission structures have recently been reported [35]. However, after investigation, we found that the bright solitons and the effect of perturbation functions on the soliton transmission process controlled by this variable coefficient (3 + 1)-dimensional CNLSEs have not been studied.

The composition of this paper is divided into the following sections: The derivation of the bilinear forms and the bright analytical solutions of System (3) will be presented in the second part. In the third part, the intensity, velocity and phase during the soliton transmission process on the planes in different directions are analyzed. Further, the influences of perturbation variable parameters on the soliton transmission process and the special phenomena will be explored. Finally, in the fourth part, the final conclusion is drawn.

Material and methods

The bilinear forms of system (3)

It is difficult to directly solve nonlinear equations, so that the following rational transformations are introduced to convert the above System (3) into the bilinear forms:

$$\psi = \frac{g}{f}, \phi = \frac{h}{f}. \tag{4}$$

And then substituting the transformations (4) into System (3), we can get the following expressions:

$$\begin{aligned} &i\frac{D_t g\cdot f}{f^2} + \beta(t)\left[\frac{D_x^2 g\cdot f + D_y^2 g\cdot f + D_z^2 g\cdot f}{f^2} - \frac{g}{f}\,\frac{D_x^2 f\cdot f + D_y^2 f\cdot f + D_z^2 f\cdot f}{f^2}\right] + \delta(t)\frac{g}{f}\left[\frac{gg^* + hh^*}{f^2}\right] = 0, \\ &i\frac{D_t h\cdot f}{f^2} + \gamma(t)\left[\frac{D_x^2 h\cdot f + D_y^2 h\cdot f + D_z^2 h\cdot f}{f^2} - \frac{h}{f}\,\frac{D_x^2 f\cdot f + D_y^2 f\cdot f + D_z^2 f\cdot f}{f^2}\right] + \omega(t)\frac{h}{f}\left[\frac{gg^* + hh^*}{f^2}\right] = 0. \end{aligned} \tag{5}$$

here f is a real function, while g and h are both complex with the variables of x, y, z and t. $''*''$ represents the conjugate symbol. And the D operator knowns as the bilinear derivative operator in the above, which is defined as follows [36,37]:

$$D_x^l D_t^m g(x,t)\cdot f(x,t) = \frac{\partial^l}{\partial a^l}\frac{\partial^m}{\partial b^m} g(x+a,t+b)f(x-a,t-b)\Big|_{a=0,b=0}(l,m=0,1,2,\cdots). \tag{6}$$

By setting $\left(D_x^2+D_y^2+D_z^2\right)f\cdot f=\mu(gg^*+hh^*)$ (μ is a positive constant) we can obtain:

$$i\frac{D_t g\cdot f}{f^2}+\beta(t)\left[\frac{D_x^2 g\cdot f+D_y^2 g\cdot f+D_z^2 g\cdot f}{f^2}\right]+[\delta(t)-\mu\beta(t)]\frac{g}{f}\left[\frac{gg^*+hh^*}{f^2}\right]=0,$$
$$i\frac{D_t h\cdot f}{f^2}+\gamma(t)\left[\frac{D_x^2 h\cdot f+D_y^2 h\cdot f+D_z^2 h\cdot f}{f^2}\right]+[\omega(t)-\mu\gamma(t)]\frac{h}{f}\left[\frac{gg^*+hh^*}{f^2}\right]=0.$$

To balance the dispersion terms and nonlinear terms, we have the constraints $\delta(t)=\mu\beta(t)$ and $\omega(t)=\mu\gamma(t)$. Since the denominator f^2 cannot be 0, we can get:

$$iD_t g\cdot f+\beta(t)[D_x^2 g\cdot f+D_y^2 g\cdot f+D_z^2 g\cdot f]=0,$$

$$iD_t h\cdot f+\gamma(t)[D_x^2 h\cdot f+D_y^2 h\cdot f+D_z^2 h\cdot f]=0$$

From the above process, the bilinear forms of system (3) are:

$$\begin{aligned}&\left[iD_t+\beta(t)(D_x^2+D_y^2+D_z^2)\right]g\cdot f=0,\\&\left[iD_t+\gamma(t)(D_x^2+D_y^2+D_z^2)\right]h\cdot f=0,\\&\left[D_x^2+D_y^2+D_z^2\right]f\cdot f-\mu(gg^*+hh^*)=0.\end{aligned}\tag{7}$$

The One-soliton solutions of System (3)

Next, the bright one-soliton solutions of System (3) will be derived according to the expansions of g and f with respect to formal parameter ξ.

$$\begin{aligned}&g=\xi g_1+\xi^3 g_3+\xi^5 g_5+\cdots,\\&h=\xi h_1+\xi^3 h_3+\xi^5 h_5+\cdots,\\&f=1+\xi^2 f_2+\xi^4 f_4+\xi^6 f_6+\cdots.\end{aligned}\tag{8}$$

when deriving the one-soliton solutions, the above expansions need to be truncated into $g=\xi g_1, h=\xi h_1$ and $f=1+\xi^2 f_2$. Making assumptions that $g_1=Ae^{\eta}, h_1=Be^{\eta}, f_2=m_1 e^{\eta+\eta^*}, \eta=\chi x+\nu y+\zeta z+k(t)$, and substituting the assumptions and the truncated expansions into the bilinear Eq. (7), the following relationships can be yielded:

$$\beta(t)=\gamma(t), k(t)=\int i(\chi^2+\nu^2+\zeta^2)\beta(t)dt,$$
$$m_1=\frac{\left(|A|^2+|B|^2\right)\mu}{2[(\chi+\chi^*)+(\nu+\nu^*)^2+(\zeta+\zeta^*)^2]}.$$

For convenience, make the assumption that $\xi=1$, so the one-soliton solutions of System (3) can be written in the following forms:

$$\psi=\frac{Ae^{\eta}}{1+\frac{\left(|A|^2+|B|^2\right)\mu}{2[(\chi+\chi^*)+(\nu+\nu^*)^2+(\zeta+\zeta^*)^2]}e^{\eta+\eta^*}},$$
$$\phi=\frac{Be^{\eta}}{1+\frac{\left(|A|^2+|B|^2\right)\mu}{2[(\chi+\chi^*)+(\nu+\nu^*)^2+(\zeta+\zeta^*)^2]}e^{\eta+\eta^*}}. \tag{9}$$

The two-soliton solutions of System (3)

When deriving the two-soliton solutions, the expansions (7) should be truncated to $g=\xi g_1+\xi^3 g_3, h=\xi h_1+\xi^3 h_3$ and $f=1+\xi^2 f_2+\xi^4 f_4$. Then, g_1 and h_1 are set to $g_1=C_1 e^{\eta_1}+C_2 e^{\eta_2}$ and $h_1=A_1 e^{\eta_1}+A_2 e^{\eta_2}$, respectively. Here, $\eta_j=\chi_j x+\nu_j y+\zeta_j z+k_j(t)$, $(j=1,2)$. Taking the above assumptions into the bilinear equations (7), we can acquire the following results:

$$\beta(t)=\gamma(t), k_j(t)=\int i\left(\chi_j^2+\nu_j^2+\zeta_j^2\right)\beta(t)dt\ (j=1,2),$$
$$g_3=B_1 e^{\eta_1+\eta_2+\eta_1^*}+B_2 e^{\eta_1+\eta_2+\eta_2^*}, h_3=F_1 e^{\eta_1+\eta_2+\eta_1^*}+F_2 e^{\eta_1+\eta_2+\eta_2^*},$$
$$f_2=M_1 e^{\eta_1+\eta_1^*}+M_2 e^{\eta_1+\eta_2^*}+M_3 e^{\eta_2+\eta_1^*}+M_4 e^{\eta_2+\eta_2^*}, f_4=n_1 e^{\eta_1+\eta_2+\eta_1^*+\eta_2^*},$$

where

$$\chi_2=\frac{\chi_1^*(\zeta_2-\zeta_1)+\chi_1(\zeta_1^*+\zeta_2)}{\zeta_1+\zeta_1^*}, \nu_2=\frac{\nu_1^*(\zeta_2-\zeta_1)+\nu_1(\zeta_1^*+\zeta_2)}{\zeta_1+\zeta_1^*},$$
$$M_1=\frac{\mu\left(|A_1|^2+|C_1|^2\right)}{2[(\chi_1+\chi_1^*)^2+(\nu_1+\nu_1^*)^2+(\zeta_1+\zeta_1^*)^2]},$$

$$M_2=\frac{\mu(A_1A_2^*+C_1C_2^*)}{2[(\chi_1+\chi_2^*)^2+(\nu_1+\nu_2^*)^2+(\zeta_1+\zeta_2^*)^2]},$$
$$M_3=\frac{\mu(A_1^*A_2+C_1^*C_2)}{2[(\chi_1^*+\chi_2)^2+(\nu_1^*+\nu_2)^2+(\zeta_1^*+\zeta_2)^2]},$$

$$M_4=\frac{\mu(|A_2|^2+|C_2|^2)}{2[(\chi_2+\chi_2^*)^2+(\nu_2+\nu_2^*)^2+(\zeta_2+\zeta_2^*)^2]},$$
$$B_1=-C_2M_1\sigma_1+C_1M_3\sigma_2, B_2=-C_2M_2\sigma_3+C_1M_4\sigma_4,$$
$$F_1=-A_2M_1\sigma_1+A_1M_3\sigma_2, F_2=-A_2M_2\sigma_3+A_1M_4\sigma_4,$$
$$n_1=\frac{-2M_1M_4\Lambda_1-2M_2M_3\Lambda_2+\mu\Lambda_4}{2\Lambda_3},$$
$$\sigma_1=\frac{(\chi_1+\chi_1^*)(\chi_1-\chi_2)+(\nu_1+\nu_1^*)(\nu_1-\nu_2)+(\zeta_1+\zeta_1^*)(\zeta_1-\zeta_2)}{(\chi_1+\chi_1^*)(\chi_1^*+\chi_2)+(\nu_1+\nu_1^*)(\nu_1^*+\nu_2)+(\zeta_1+\zeta_1^*)(\zeta_1^*+\zeta_2)},$$
$$\sigma_2=\frac{(\chi_1^*+\chi_2)(\chi_1-\chi_2)+(\nu_1^*+\nu_2)(\nu_1-\nu_2)+(\zeta_1^*+\zeta_2)(\zeta_1-\zeta_2)}{(\chi_1+\chi_1^*)(\chi_1^*+\chi_2)+(\nu_1+\nu_1^*)(\nu_1^*+\nu_2)+(\zeta_1+\zeta_1^*)(\zeta_1^*+\zeta_2)},$$
$$\sigma_3=\frac{(\chi_1+\chi_2^*)(\chi_1-\chi_2)+(\nu_1+\nu_2^*)(\nu_1-\nu_2)+(\zeta_1+\zeta_2^*)(\zeta_1-\zeta_2)}{(\chi_1+\chi_2^*)(\chi_2+\chi_2^*)+(\nu_1+\nu_2^*)(\nu_2+\nu_2^*)+(\zeta_1+\zeta_2^*)(\zeta_2+\zeta_2^*)},$$
$$\sigma_4=\frac{(\chi_1-\chi_2)(\chi_2+\chi_2^*)+(\nu_1-\nu_2)(\nu_2+\nu_2^*)+(\zeta_1-\zeta_2)(\zeta_2+\zeta_2^*)}{(\chi_1+\chi_2^*)(\chi_2+\chi_2^*)+(\nu_1+\nu_2^*)(\nu_2+\nu_2^*)+(\zeta_1+\zeta_2^*)(\zeta_2+\zeta_2^*)},$$
$$\Lambda_1=(\chi_1+\chi_1^*-\chi_2-\chi_2^*)^2+(\nu_1+\nu_1^*-\nu_2-\nu_2^*)^2+(\zeta_1+\zeta_1^*-\zeta_2-\zeta_2^*)^2,$$
$$\Lambda_2=(\chi_1-\chi_1^*-\chi_2+\chi_2^*)^2+(\nu_1-\nu_1^*-\nu_2+\nu_2^*)^2+(\zeta_1-\zeta_1^*-\zeta_2+\zeta_2^*)^2,$$
$$\Lambda_3=(\chi_1+\chi_1^*+\chi_2+\chi_2^*)^2+(\nu_1+\nu_1^*+\nu_2+\nu_2^*)^2+(\zeta_1+\zeta_1^*+\zeta_2+\zeta_2^*)^2,$$
$$\Lambda_4=B_2^*C_1+B_2C_1^*+B_1^*C_2+B_1C_2^*+A_2^*F_1+A_2F_1^*+A_1^*F_2+A_1F_2^*.$$

Without loss of generality, assuming $\xi=1$, then the expressions of the bright two-soliton solutions are as follows:

$$\psi=\frac{g_1+g_3}{1+f_2+f_4}, \phi=\frac{h_1+h_3}{1+f_2+f_4} \tag{10}$$

Results discussion

To explore the traits of the velocity and intensity in solitons transmission process controlled by this model, for intuitive analysis, the above-mentioned one-soliton solutions (9) are transformed as follows:

$$\begin{aligned}\psi &=\frac{g_1}{1+f_2}=\frac{A}{2}e^{i\mathrm{Im}(\eta)}e^{-\frac{\ln m_1}{2}}\mathrm{sech}\left[\mathrm{Re}(\eta)+\frac{\ln m_1}{2}\right],\\ \phi &=\frac{h_1}{1+f_2}=\frac{B}{2}e^{i\mathrm{Im}(\eta)}e^{-\frac{\ln m_1}{2}}\mathrm{sech}\left[\mathrm{Re}(\eta)+\frac{\ln m_1}{2}\right].\end{aligned}\tag{11}$$

where $Re(\eta)$ and $Im(\eta)$ represent the real and imaginary parts of η, respectively. The characteristic-line equation (12) is introduced in the soliton transmission process to convey the expression of transmission speed [38].

$$Re(\eta)+\frac{1}{2}\ln m_1=const. \tag{12}$$

Assuming $\chi = X_{11} + iX_{12}$, $v = Y_{11} + iY_{12}$, $\zeta = Z_{11} + iZ_{12}, X_{1j}, Y_{1j}, Z_{1j}$ are real constants and $j = 1, 2$, then substituting them into Eq. (12), the following relationship is obtained:

$$X_{11}x + Y_{11}y + Z_{11}z - 2(X_{11}X_{12} + Y_{11}Y_{12} + Z_{11}Z_{12}) \int \beta(t)dt + \frac{1}{2}lnm_1 = const. \tag{13}$$

Differentiate on both sides of Eq. (13), therefore, the soliton transmission velocity in the $x - t$, $y - t$, and $z - t$ planes are inferred:

$$v_{x-t} = \frac{2(X_{11}X_{12} + Y_{11}Y_{12} + Z_{11}Z_{12})\beta(t)}{X_{11}},$$
$$v_{y-t} = \frac{2(X_{11}X_{12} + Y_{11}Y_{12} + Z_{11}Z_{12})\beta(t)}{Y_{11}},$$
$$v_{z-t} = \frac{2(X_{11}X_{12} + Y_{11}Y_{12} + Z_{11}Z_{12})\beta(t)}{Z_{11}}.$$

It is shown that the transmission speed of the soliton is affected by wave numbers χ, v, ζ and disturbance coefficient$\beta(t)$. What's more, under the same parameter conditions, the larger the real value of the wave numbers of each plane, the smaller the velocity of the plane. As can be seen from Fig. 1(a) and (b), in the $x - t$ plane, the soliton transmission velocity does not increase or decrease for the changes about the values of y and z, but its transmission position is shifted to the right. It is because the values of y and z will affect the initial phase of the soliton in the $x - t$ plane transmission. On the other hand, comparing the soliton transmission velocity on different planes from Fig. 1(a), (b) and (c), as the real part values of χ, v, and ζ are $0.5, 1$, and 1.5, respectively, we can see that the speed of Fig. 1 (a) is the largest, and Fig. 1 (c) is the smallest, which confirms the expressions of v_{x-t}, v_{y-t} and v_{z-t} from the image aspect.

Next, we continue to discuss some special phenomena caused by the effects of perturbation parameters $\beta(t)$ on soliton transmission. When $\beta(t)$ takes a constant, the solitons are linear on the corresponding plane in Fig. 1, but once $\beta(t)$ takes different functions, it will have different shapes on the corresponding plane. For instance, in the $x - t$ plane, when $\beta(t)$ takes $0.5e^t$ or t^2, the solitons appear parabolic in Fig. 2(a) and (b). But if we suppose $\beta(t) = \lambda tan(\rho t)$, there will be a periodic parabolic soliton with different energies in Fig. 2(c) and (d). Not only that, the purpose of changing the period and span of the parabolic solitons can be achieved by adjusting the parameters λ and ξ. $\beta(t)$ can take various functions, when $\beta(t)$ is taken as t^2, $0.2sin(2t)$, $sech(5t)$, $0.05t^2sin(t)$, respectively, cubic (Fig. 2(e)), sine (Fig. 2(f)), hyperbolic sine (Fig. 2 (g)) and periodic increased amplitude(Fig. 2(h)) solitons are obtained.

According to Eq. (11), the intensities of ψ and ϕ are as follows:

$$|\psi|^2 = \frac{|A|^2}{4m_1} sech^2[Re(\eta) + \tfrac{1}{2}lnm_1],$$
$$|\phi|^2 = \frac{|B|^2}{4m_1} sech^2[Re(\eta) + \tfrac{1}{2}lnm_1].$$

Because $sech(x) \le 1$, there is

$$|\psi|^2_{max} = \frac{|A|^2}{4m_1} = \frac{(\chi+\chi^*)+(v+v^*)^2+(\zeta+\zeta^*)^2}{2\left(1+\frac{|B|^2}{|A|^2}\right)\mu},$$
$$|\phi|^2_{max} = \frac{|B|^2}{4m_1} = \frac{(\chi+\chi^*)+(v+v^*)^2+(\zeta+\zeta^*)^2}{2\left(1+\frac{|A|^2}{|B|^2}\right)\mu}.$$

The above equations show that the intensity of the soliton is not related to the constraint parameter $\beta(t)$, but is related to X, Y, Z, the phase constant A and B, and the parameter μ. Further, when $|\frac{A}{B}|$ increases, the intensity of ψ increases but ϕ decreases.

Next, we will concentrate on discussing the interactions of the two-solitons in System (3). From Eq. (11), we know that the difference between ψ and ϕ is only proportional to the energy, so the following discussion about the soliton's interactions is only for ψ. As we can see, under certain parameters values, by adjusting the wave number parameters χ_j, v_j and ζ_j, solitons appear to merge, split and deform in the process of interaction. In Fig. 3 (a), the two solitons are fused into a single soliton with greater intensity and wider wave width. However, when the parameters values become $Z_1 = 1.2 - 0.38I, Y_1 = -0.91 + 0.5I$, the two solitons do not merge. Instead, one of the solitons absorbed the energy of the other soliton, and the intensity and wave width increased, on the other hand, the energy and wave width of the other soliton are reduced in Fig. 3 (b). The energy and waveform of the solitons have changed after the interaction, which is an inelastic interaction caused by energy redistribution. Further, by adjusting the values of Y_1 and Z_1, the two-solitons are split, and side wave appear. A new soliton is formed between the two solitons, and its energy is greater than that of the two solitons in Fig. 3 (c). Fig. 3 (d) is the cases where the two-solitons split into four waves. This kind of interaction that will generate new solitons may be beneficial to quickly improve the efficiency of optical communications. In addition to fusion and splitting, the two- solitons of System (3) will undergo severe deformation in the area of interaction in Fig. 3(e) and (f). This phenomenon will reduce the accuracy of information transmission and is also a problem that must be solved to improve the transmission efficiency of optical fibers.

Finally, parameters v_j and ζ_j can also modulate the synchronization of soliton transmissions. The propagation of optical soliton in a dispersion-graded fiber is similar to a sinusoidal curve. Therefore, $\beta(t)$ is taken as a sine function to simulate the transmission process of a soliton in a dispersion graded fiber. As can be seen in Fig. 4 (a),

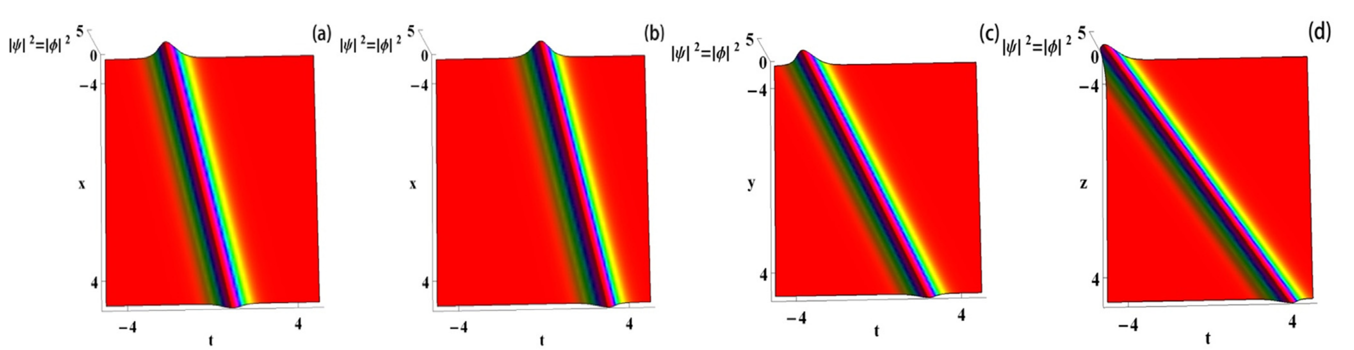

Fig. 1. The velocity comparison on different planes of one-soliton solitons, corresponding parameters are: $\beta(t) = 0.3, \mu = 1, A = 1 + I, B = 1 + I, \chi = 0.5 + I, v = 1 + I, \zeta = 1.5 + I, (a) y = 0, z = 0; (b) y = 2, z = 1; (c) x = 0, z = 0; (d) x = 0, y = 0.$

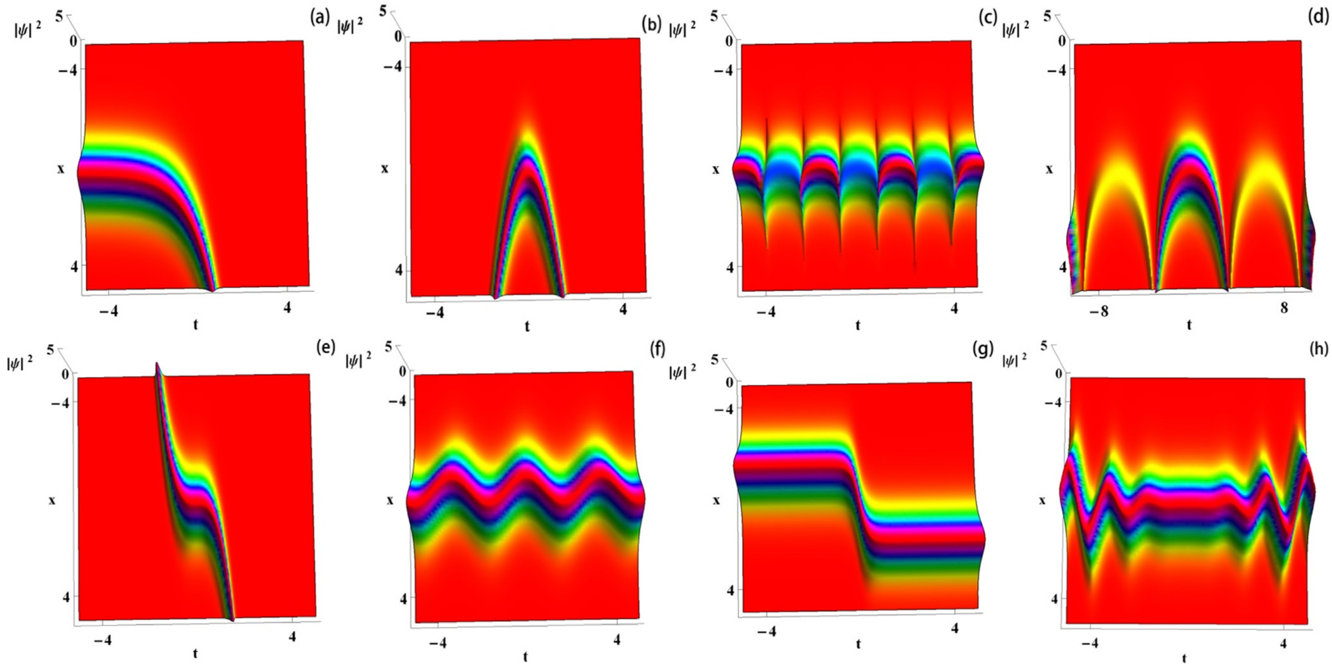

Fig. 2. The different shapes of solitons generate on the $x - t$ plane by $\beta(t)$: $A = -2 + I, B = 1 + I, \chi = 1 + I, v = 0.5 + I, \zeta = 1 + I, y = 0, z = 0$, (a) $\beta(t) = 0.5e^t, \mu = 1$; (b) $\beta(t) = t, \mu = 1$; (c) $\beta(t) = 0.1tan(2t), \mu = 1.5$; (d) $\beta(t) = 0.2tan(0.5t), \mu = 1$; (e) $\beta(t) = t^2, \mu = 1$; (f) $\beta(t) = 0.2sin(2t), \mu = 1$; (g) $\beta(t) = sech(5t), \mu = 1$; (h) $\beta(t) = 0.05t^2 sin(4t), \mu = 1$.

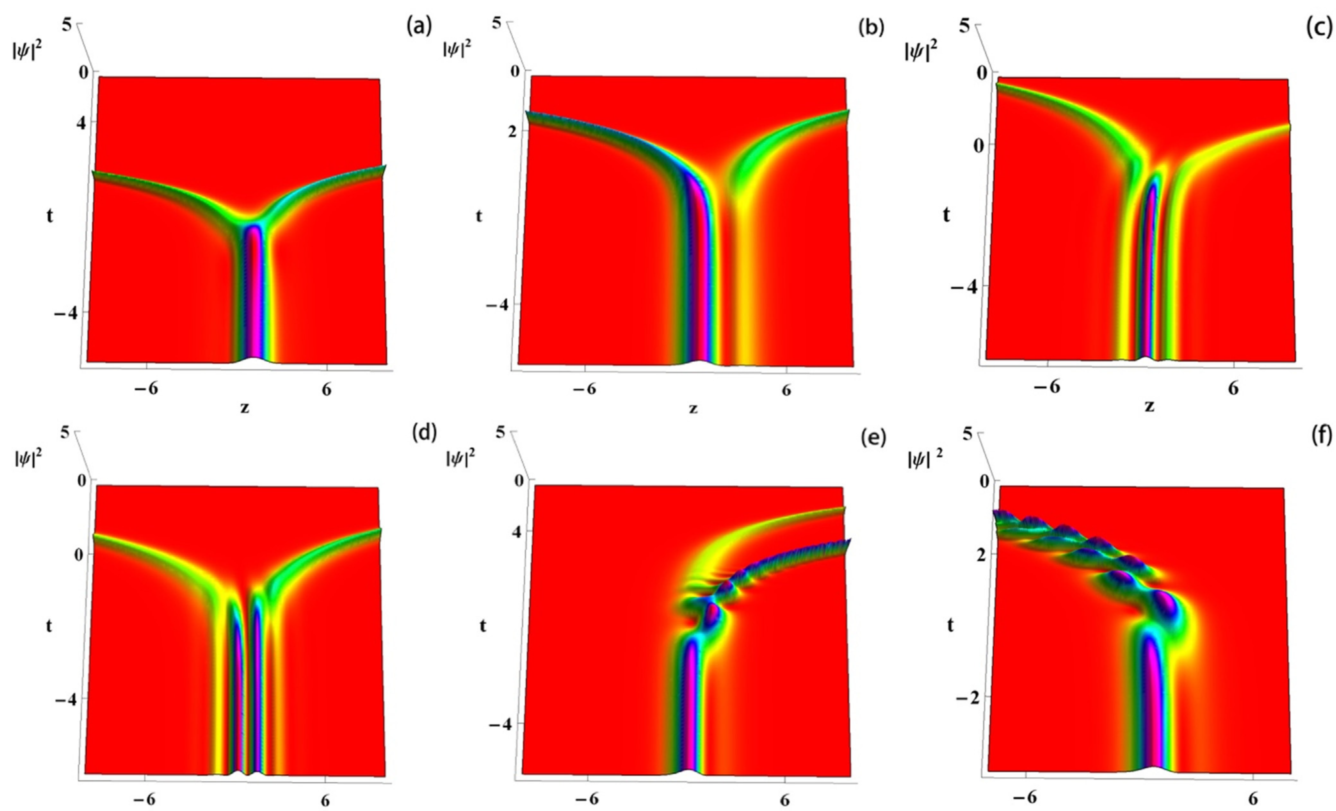

Fig. 3. Two-soliton interactions with different constraint coefficients: $\beta(t) = e^t, \mu = 2, A_1 = -1, A_2 = 1, C_1 = 1, C_2 = 1, \chi_1 = 0.3 + I, \zeta_2 = 1 + 0.1I, x = 1, y = 1$, (a) $\zeta_1 = -1.2 + 1.1I$, $v_1 = 1.0 + 0.19I$, (b) $\zeta_1 = 1.2 - 0.38I, v_1 = -0.91 + 0.5I$, (c) $\zeta_1 = -0.81 + 3.5I, v_1 = -0.0663 - 2.8I$, (d) $\zeta_1 = 0.81 - 4I, v_1 = -0.44 - 0.38I$, (e) $\zeta_1 = 1.9 + 0.25I$, $v_1 = 0.13 - 3.2I$, (f) $\zeta_1 = 1.6 + 0.13I, v_1 = -0.88 + 1.1I$.

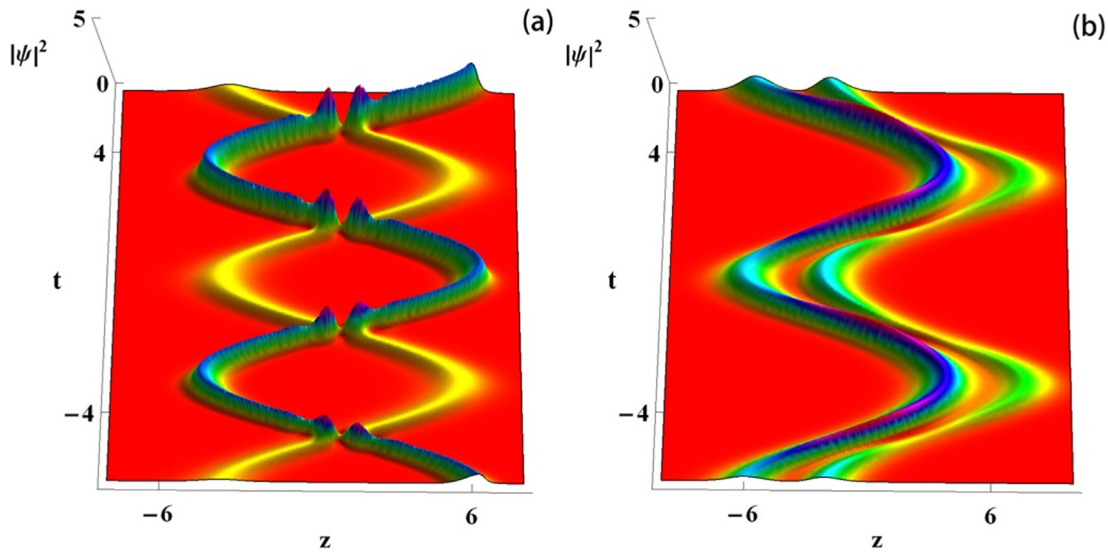

Fig. 4. Two-soliton interactions with different constraint coefficients: $\beta(t) = sint, \mu = 2, A_1 = -1, A_2 = 1, C_1 = 1, C_2 = 1, \chi_1 = 0.3 + I, \zeta_2 = 1 + 0.1$, (a) $\zeta_1 = 2 - 3.8I, \nu_1 = -0.94 - 2.3I, x = 1, y = 1$; (b) $\zeta_1 = 0.88 + 0.5I, \nu_1 = -1.1 - 1.7I, x = -1, y = -1$.

the two solitons are sinusoidal waves under the action of $\beta(t)$, and the vibration directions of the two solitons are opposite. However, with different values of ζ_1 and ν_1, the vibration directions of the two solitons become synchronized in Fig. 4 (b). From the previous analysis in Fig. 1(a) and (b), it is known that only the transmission positions of the solitons are different on the different planes in the same direction. Therefore, it can be known from Fig. 4 that the inconsistencies of the sine-wave soliton can be achieved by adjusting parameters ζ_1 and ν_1. So that the wave number parameters can not only manage the shape and energy of the solitons themselves, but also modulate the coordination of the two-solitons during the transmissions. At the same time, in Fig. 4, the two solitons only locally deform in the interaction range, and after the interaction, the shape does not change. Thus, the interactions are elastic interactions which has less impact on information transmission during the fiber transmission process.

Conclusion

In this paper, we have investigated a variable coefficient (3 + 1)-dimensional CNLSE (3) describing circularly polarized waves. The Horita's method have been used to transform Eq. (3) into the bilinear forms, and the bright one- and two-soliton solutions have been derived. After some derivations, the expressions of soliton transmission velocity and intensity have been obtained. It can be known from the expressions of velocity that in addition to the parameters χ, ν, and ζ, the transmission volecity has been controlled by the disturbance coefficient $\beta(t)$. Moreover, when $\beta(t)$ has took different functions, soliton transmission paths of different shapes have appeared on the corresponding plane. On the other hand, the intensity of the solitons has been affected by the parameter χ, ν, ζ, and μ. Since the parameters χ_1, ν_1 and ζ_j affect the speed and intensity of the solitons, it is inevitable that the interactions of the solitons would be affected by them in the transmissions. Constantly adjusting the parameters ν_1 and ζ_1, it was found that the two solitons had fused, split and deformed. And under certain conditions, the energy of one soliton would be absorbed by the other soliton. In the process of soliton fusion and splitting, both belong to inelastic interactions caused by energy redistribution. Finally, we have found that during the sinusoidal two-soliton transmission, the parameters ν_1 and ζ_1 can adjust the vibrations synchronization of the two-solitons. This shows that the transmission path and state of the soliton can be controlled by controlling the adjustable parameters.

Compliance with ethics requirements

This article does not contain any studies with human or animal subjects.

Declaration of Competing Interest

The authors declare that they have no known competing financial interests or personal relationships that could have appeared to influence the work reported in this paper.

Acknowledgements

The work of Wenjun Liu was supported by the National Natural Science Foundation of China (NSFC) (Grants 11705130, 11674036 and 11875008), Beijing Youth Top Notch Talent Support Program (Grant 2017000026833ZK08), Fund of State Key Laboratory of Information Photonics and Optical Communications (Beijing University of Posts and Telecommunications, Grant IPOC2019ZZ01), Fundamental Research Funds for the Central Universities (Grant 500419305). This project was funded by the Deanship of Scientific Research (DSR), King Abdulaziz University, Jeddah, Saudi Arabia, under Grant No. (KEP-65-130-38). The authors, therefore, acknowledge with thanks DSR technical and financial support.

References

[1] Li M, Xu T. Dark and anti-dark soliton interactions in the nonlocal nonlinear Schrödinger equation with the self-induced parity-time-symmetric potential. Phys Rev E 2015;91:. https://doi.org/10.1103/PhysRevE.91.033202 033202.

[2] Ma LY, Zhu ZN. N-soliton solution for an integrable nonlocal discrete focusing nonlinear Schrödinger equation. Appl Math Lett 2016;59:115–21. https://doi.org/10.1016/j.aml.2016.03.018.

[3] Quintero NR, Mertens FG, Bishop AR. Soliton stability criterion for generalized nonlinear Schrödinger equations. Phys Rev E 2015;91:. https://doi.org/10.1103/PhysRevE.91.012905012905.

[4] Yan YY, Liu WJ. Stable transmission of solitons in the complex cubic-quintic Ginzburg-Landau equation with nonlinear gain and higher-order effects. Appl Math Lett 2019;98:171–6. https://doi.org/10.1016/j.aml.2019.06.008.
[5] Liu WJ, Zhang Y, Wazwaz AM, Zhou Q. Analytic study on triple-S, triple-triangle structure interactions for solitons in inhomogeneous multi-mode fiber. Appl Math Comput 2019;361:325–31. https://doi.org/10.1016/j.amc.2019.05.046.
[6] Guan X, Liu WJ, Zhou Q, Biswas A. Darboux transformation and analytic solutions for a generalized super-NLS-mKdV equation. Nonlinear Dyn 2019;98:1491–500. https://doi.org/10.1007/s11071-019-05275-0.
[7] Liu SZ, Zhou Q, Biswas A, Liu W. Phase-shift controlling of three solitons in dispersion-decreasing fibers. Nonlinear Dyn 2019;98:395–401. https://doi.org/10.1007/s11071-019-05200-5.
[8] Liu XY, Liu WY, Triki H, Zhou Q, Biswas A. Periodic attenuating oscillation between soliton interactions for higher-order variable coefficient nonlinear Schrödinger equation. Nonlinear Dyn 2019;96:801–9. https://doi.org/10.1007/s11071-019-04822-z.
[9] Gao XY, Guo YJ, Shan WR. Water-wave symbolic computation for the earth, enceladus and titan: The higher-order Boussinesq-Burgers system, auto- and non-auto-Backlund transformations. Appl Math Lett 2020;104:. https://doi.org/10.1016/j.aml.2019.106170106170.
[10] Du Z, Tian B, Chai HP, Zhao XH. Dark-bright semi-rational solitons and breathers for a higher-order coupled nonlinear Schrodinger system in an optical fiber. Appl Math Lett 2020;102:. https://doi.org/10.1016/j.aml.2019.106110106110.
[11] Zhang HQ, Liu XL, Wen LL. Soliton, breather, and rogue wave for a (2+1)-dimensional nonlinear Schrödinger equation. Z Naturforsch C 2015;71:95–101. https://doi.org/10.1515/zna-2015-0408.
[12] Wang XM, Zhang LL. The nonautonomous N-soliton solutions for coupled nonlinear Schrödinger equation with arbitrary time-dependent potential. Nonlinear Dyn 2017;88:2291–302. https://doi.org/10.1007/s11071-017-3377-5.
[13] Tang B, Fan Y, Wang J. Exact solutions for N-coupled nonlinear Schrödinger equations with variable coefficients. Z Naturforsch A 2016;71:665–72. https://doi.org/10.1515/zna-2016-0128.
[14] Guan X, Liu W, Zhou Q, Biswas A. Some lump solutions for a generalized (3+1)-dimensional Kadomtsev-Petviashvili equation. Appl Math Comput 2010;366:. 0.1016/j.amc.201 9.1247 57124757.
[15] Liu WJ, Zhang Y, Luan ZT, Zhou Q, Mirzazadeh M, Ekici M, et al. Dromion-like soliton interactions for nonlinear Schrödinger equation with variable coefficients in inhomogeneous optical fibers. Nonlinear Dyn 2019;96:729–36. https://doi.org/10.1007/s11071-019-04817-w.
[16] Yang CY, Zhou Q, Triki H, Mirzazadeh M, Ekici M, Liu WJ, et al. Bright soliton interactions in a (2+1)-dimensional fourth-order variable-coefficient nonlinear Schrödinger equation for the Heisenberg ferromagnetic spin chain. Nonlinear Dyn 2019;95:983–94. https://doi.org/10.1007/s11071-018-4609-z.
[17] Du XX, Tian B, Qu QX, Yuan YQ, Zhao XH. Lie group analysis, solitons, self-adjointness and conservation laws of the modified Zakharov-Kuznetsov equation in an electron-positron-ion magnetoplasma. Chaos Solitons Fract 2020;134:. https://doi.org/10.1016/j.chaos. 2020.109709109709.
[18] Xu T, Li J, Zhang HQ. Integrable aspects and applications of a generalized inhomogeneous N-coupled nonlinear Schrödinger system in plasmas and optical fibers via symbolic computation. Phys Lett A 2008;372:1990–2001. https://doi.org/10.1016/j.physleta.2007.10.068.
[19] Ostrovskaya EA, Kivshar YS, Lisak M, Hall B, Cattani F, Anderson D. Coupled-mode theory for Bose-Einstein condensates. Phys Rev A 2000;61. https://doi.org/10.1103/physreva.61.031601.
[20] Yang Q, Zhang JF. Bose-Einstein solitons in time-dependent linear potential. Opt Commun 2006;258:35–42. https://doi.org/10.1016/j.optcom.2005.07.047.
[21] Sun WR, Tian B, Wang YF. Soliton excitations and interactions for the three-coupled fourth-order nonlinear Schrödinger equations in the alpha helical proteins. Eur Phys J D 2015;69:146. https://doi.org/10.1140/epjd/e2015-60027-6.
[22] Boyd RW. Nonlinear optics. San Diego: Academic Press; 1992.
[23] Mansfield EL, Reid GJ, Clarkson PA. Nonclassical reductions of a (3+1)-cubic nonlinear Schrödinger system. Comput Phys Commun 1998;115:460. https://doi.org/10.1016/S0010-4655(98)001 36-2.
[24] Mollenauer LF, Evangelides SG, Gordon JP. Wavelength division multiplexing with solitons in ultra-long transmission using lumped amplifiers. J Lightwave Technol 1991;9:362–7. https://doi.org/10.1109/50.70013.
[25] Chakravarty S, Ablowitz MJ, Sauer JR. Multisoliton interactions and wavelength-division multiplexing. Opt Lett 1995;20:136–8. https://doi.org/10.1364/OL.20.000136.
[26] Radhakrishnan R, Lakshmanan M. Bright and dark soliton solutions to coupled nonlinear Schrödinger equations. J. Phys. A 1999;28:2683. https://doi.org/10.1088/0305-4470/28/9/025.
[27] Kanna T, Lakshmanan M. Exact soliton solutions, shape changing collisions, and partially coherent solitons in coupled nonlinear Schrödinger equations. Phys Rev Lett 2001;86:5043–6. https://doi.org/10.1103/PhysRevLett.86.5043.
[28] Zhang HQ, Meng XH, Xu T, Li LL, Tian B. Interactions of bright solitons for the (2+1)-dimensional coupled nonlinear Schrödinger equations from optical fibers with symbolic computation. Phys Scr 2007;75:537–42. https://doi.org/10.1088/0031-8949/75/4/028.
[29] Wang YP, Tian B, Sun WR, Liu DY. Analytic study on the mixed-type solitons for a (2+1)-dimensional N-coupled nonlinear Schrödinger system in nonlinear optical-fiber communication. Commun. Nonlinear Sci 2015;22:1305–12. https://doi.org/10.1016/j.cnsns.2014.07.029.
[30] Su JJ, Gao YT. Dark solitons for a (2+1)-dimensional coupled nonlinear Schrödinger system with time-dependent coefficients in an optical fiber. Superlattice Microst 2017;104:498–508. https://doi.org/10.1016/j.spmi.2016.12.056.
[31] Yu WT, Liu WJ, Triki H, Zhou Q, Biswas A, Belic MR. Control of dark and anti-dark solitons in the (2+1)-dimensional coupled nonlinear Schrödinger equations with perturbed dispersion and nonlinearity in a nonlinear optical system. Nonlinear Dyn 2019;97:471–83. https://doi.org/10.1007/s11071-019-04992-w.
[32] Chen SS, Tian B, Sun Y, Zhang CR. Generalized darboux transformations, rogue waves, and modulation instability for the coherently coupled nonlinear Schrodinger equations in nonlinear optics. Ann Phys (Berlin) 2019;531:1900011. https://doi.org/10.1002/andp.201900011.
[33] Huang Z, Xu J, Sun B. A new solution of Schrödinger equation based on symplectic algorithm. Comput Math Appl 2015;69:1303–12. https://doi.org/10.1016/j.camwa.2015.02.025.
[34] Zhong ZL. Dark solitonic interactions for the (3+1)-dimensional coupled nonlinear Schrödinger equations in nonlinear optical fibers. Opt Laser Technol 2019;113:462–6. https://doi.org/10.1016/j.optlastec.2018.12.040.
[35] Yu WT, Liu WJ, Triki H, Zhou Q, Biswas A. Phase shift, oscillation and collision of the anti-dark solitons for the (3+1)-dimensional coupled nonlinear Schrödinger equation in an optical fiber communication system. Nonlinear Dyn 2019;97:1253–62. https://doi.org/10.1007/s11071-019-05 045-y.
[36] Hirota R. Exact envelope-soliton solutions of a nonlinear wave equation. J Math Phys 1973;14:805. https://doi.org/10.1063/1.1666399.
[37] Hirota R, Ohta Y. Hierarchies of coupled soliton equations. I, J Phys Soc Jpn 1991;60:798–809. https://doi.org/10.1143/JPSJ.60.798.
[38] Yang JW, Gao YT, Wang QM. Bilinear forms and soliton solutions for a fourth-order variable coefficient nonlinear Schrödinger equation in an inhomogeneous Heisenberg ferromagnetic spin chain or an alpha helical protein. Phys B 2016;481:148–55. https://doi.org/10.1016/j.physb.2015.10.025.